

Characterization of Dissimilar Alloys Welding Techniques with Enhanced Galvanic Corrosion

¹Husnain Shabir, ^{1,2}Khalid. H. Hashmi, ¹Ghulam Zakria,
²Shahid Khalil, ¹Mahboob Alam and ³Muhammad Farooq

¹Advanced Engineering Research Organization, HasanAbdal, Wah Cantt, Pakistan

²University of Engineering and Technology Taxila, Pakistan

³Government Swedish-Pakistan Institute of Technology, Gujrat, Pakistan

Abstract: In recent era, requirement for joining dissimilar alloys is increasing gradually. A lot of benefits are acquired by welding dissimilar alloys. Better and hybrid properties can be obtained with reduced overall cost. In present research work, sheets of AISI 304 which is an austenitic stainless steel and AISI 1040 that is a medium carbon steel were joined together by using Shielded Metal Arc Welding (SMAW) and Gas Tungsten Arc Welding (GTAW) techniques. The welding joint was completed in three passes by using E-309 16 and ER-309 L welding electrodes for SMAW and GTAW respectively. Standard samples were prepared for Tensile test, Impact test, Bend test, Hardness test and Metallography from welded sheets. SMAW and GTAW joints were characterized by means of Mechanical Testing and microstructure was analyzed under Scanning Electron Microscope (SEM). It was concluded that GTAW joints possess superior qualities as compared to the SMAW joints. However, it was observed that sheet of AISI 1040 got corroded. To avoid corrosion, the welded sheets were coated by electrolytic cadmium plating. The cadmium plated samples were then tested for accelerated corrosion testing in Salt Spray Chamber for 96 hours according to the standard ASTM B117. Solution of 5 % NaCl was utilized in the Fog Test. After 96 hours no corrosion of any type was detected. Thus it is proved that GTAW welded AISI 1040 and AISI 304 materials with cadmium plating can provide optimized results and can be used for different engineering applications.

Key words: Welding • Galvanic corrosion • SMAW • GTAW • SEM • Cadmium plating • Fog Ttest

INTRODUCTION

Selection of material for manufacturing a particular product is extremely important because of design, manufacturing and economic considerations. Same materials cannot be used for every application even in the same area of application like. stainless steel (SS) with good strength, excellent corrosion resistance and attractive surface finish are available and can be used for many industrial application but at the same time it is not recommended to be used for making windows, hooks and frames because of its high cost. However, there are some specific engineering applications which require the superior properties at one end of the part as compared to the other end. In such cases the joint between two dissimilar materials becomes more significant and is commonly used now a day [1].

Dissimilar metal welding may be defined as the weldment obtained between two dissimilar kinds of materials either metals or alloys by any welding process such as welding of Al-Mg-Si and Al-Mn [2]. In dissimilar metals welding the chemical composition of the filler metal differs from the metals being welded. Joining of light weight alloys to the dense metals for transportation applications will reduce the fuel consumption [3]. Joining of different grades of alloys is necessary in nuclear power plant for design view point [4]. There are also numerous difficulties to be faced while welding of dissimilar metals, these includes the different coefficient of thermal expansion, different magnitude, direction and type of stresses induced, control of fracture, bending and creep phenomenon.

SMAW joints are more susceptible to pitting corrosion in salt spray test as compared to the GTAW joints [5]. By increasing the temperature of weld bead (WB) the fracture is transferred from the WB to base metal (BM) [1]. Precipitation hardened alloy show poor weldability by fusion welding process [6]. Cracks are formed during welding of dissimilar metals due to different coefficient of thermal expansion [7, 8]. Formation of compounds in welding of aluminum and titanium mostly depends upon travel speed by Friction Stir Welding (FSW) [9]. Hardness shows irregular pattern by FSW and maximum hardness is obtained in center of weld bead [10].

The problems occurred in joining of dissimilar metals by welding due to difference in their CTE may be overcome by adopting our proposed techniques. Better designing of welding joints can significantly reduce the stresses generated during welding. The intensity of these stresses can also be reduced by applying preheating and post heating treatments. [11]. One way to reduce stresses is to use filler rod having CTE in between the CTE of materials to be joined [10]. When two different materials are joined galvanic couple is produced between them due to the welding process and one of BM will be attacked by galvanic corrosion [12].

Dilution is a change in chemical composition of a welding filler rod due to mixing of the parent metals and previously deposited weld metals in WB. The theory of dilution is principally significant in fusion welding of different alloys. There are three different metals involved during welding of dissimilar metals. Out of these three metals, two are base metals and the third is filler metal. When welding process proceeds, both parent metals, will melt and mix with the molten filler metal [13].

Primary important reason for welding of dissimilar metals is to achieve desired properties economically but the question is that how it is possible to join these materials successfully without any defect and with enhanced service life by combating corrosion issues.

During the present research work, the sheets of AISI-1040 and AISI-304 steel are welded together by SMAW technique with a filler rod AWS, E-309 16 and GTAW technique by using a filler rod AWS, ER-309L. Samples were studied to get information about their mechanical properties like tensile strength, bending strength, fracture strength, yield strength, ductility, toughness and hardness. The microstructure of the specimen in Heat Affected Zone (HAZ) and weld zone (WZ) was studied. Electrolytic cadmium plating was performed and corrosion resistance of the joint of dissimilar alloys was studied.

Methodology: Plates of AISI 1040 and AISI 304 having dimensions 320x160x10 mm were prepared for the test experiment. The chemical composition of the material was confirmed by spark emission spectroscopy. The length of the plates was fixed 320mm for the medium carbon steel AISI 1040 and the stainless steel AISI 304. Followed by the cutting process the plates were faced and beveled in “V” shape at an angle of 60° on milling machine while the ‘face root’ value was kept 1 mm. The purpose of bevelling is to obtain complete penetration of filler metal throughout the thickness of welded plates. ‘Tacking’ was done for proper positioning, alignment and to combat welding distortion.

Two types of welding techniques SMAW and GTAW were utilized for joining AISI 1040 and AISI 304 steel. GTAW technique was used for joining the AISI 304 and AISI 1040 alloys at 1G position (welding of plate in horizontal or flat position) by using 3 passes. Pure argon gas was utilized for the purpose of shielding the base alloys and to overcome contamination problems in weld bead. Filler rod applied during the welding of SS and Medium Carbon Steel (MCS) was ER 309 L.

SMAW process was also carried out at flat position or 1-G position with D.C reverse polarity, the welding electrode for this technique was E-309 16.

During SMAW process after the complete consumption of electrode, surface of weld bead was well ground with the help of disk grinder to remove slag from the surface before starting next electrode. Slag from all over the surface of first and second pass was first chipped off before starting next pass. SMAW joint was concluded by using 3 passes.

Welded sheets were machined by the milling machine to prepare different samples for mechanical testing, during the milling operation; coolant was applied continuously to avoid the overheating of welded area of specimens. Eighteen specimens were prepared for tensile testing (9 samples for each welding technique) according to ASME IX QW 462. Tensile test was performed by using universal tensile testing machine. Gauge length was marked before starting the test, with a deformation rate of 10 mm/min.

To measure the toughness, Charpy V-notch tests were performed on Shimadzu Charpy impact testing machine with a hammer possessing 40 kg mass. Eighteen specimens (Nine for each welding technique) for impact testing were prepared according to the ASTM E-23 [15]. For impact testing V notch was made in the regions of centre of weld bead, at the interface of weld bead and AISI 304 base metal and at the interface of weld bead and

AISI 1040 base metal. Guided bend test in accordance to the ASME section-IX, [16] was carried out in longitudinal direction, in such a way that the bend was formed across the rolling direction and along the weld, with an angle of bend 180° with a deformation rate of 30 mm /minute. Six samples (three for each technique) were prepared for Face Bend test.

Micro hardness test was carried out by Vickers hardness testing machine with a square based diamond tip indenter from centre of weld bead towards the base metal by using a load of 10 kg.

Samples were prepared for Scanning Electron Microscope (SEM) by mechanical grinding and polishing. Nital was used as an etchant containing 2 ml concentrated nitric acid (HNO₃) and 98 ml of ethyl alcohol, to expose the grain boundary of ferrite & pearlite in AISI 1040 steel. Metallographic specimens were dipped in Nital for time of 4-10 seconds; minute agitation provided the best results to reveal microstructure. For AISI 304 and weldment Oxalic acid based etching agent was utilized because the Nital does not etch these materials. Etching was done right after the polishing to avoid the formation of passive layer. As HAZ is high energy area that's why it was etched at a faster rate as compared to the base metal, Etching was done in two stages first for the HAZ and thereafter to see the microstructure of base metal.

Microstructures were taken at different magnifications and regions of weld bead, heat affected zone and base metals.

To enhance the service life and corrosion resistance, Cadmium electroplating was performed. Thickness of the cadmium plating was maintained from 16-22 micron, this thickness was ensured with the help of thickness testing meter called Elcometer and it was within the specified range. Coating thickness was then verified under SEM by taking microstructure of cross sectional specimen of welded sheets.

Salt spray examination is an accelerated corrosion test that creates an artificial and accelerated corrosive attack environment on the plated components and is utilized to forecast its fitness in service as a defensive surface finish. Four samples were prepared for salt spray. Among four samples two for each welding technique were

taken after polishing without cadmium plating and the other two were after cadmium plating. Salt spray test for corrosion examination was performed in a closed testing chamber, containing a 5% solution of NaCl recognized as NSS (neutral salt spray). Corrosion was observed on the samples after 10 hours in AISI 1040 base metal for samples those were not electroplated. Electroplated samples were placed in the salt spray chamber for a time period of 96 hours continuously and they did not show any corrosion product.

RESULTS AND DISCUSSIONS

The materials were tested by using spark emission spectroscopy to verify the chemical composition of AISI 1040 steel and AISI 304 steel. The chemical composition of the materials along with chemical composition of electrodes is shown in Table 1.

In Figure 1, linear graphs demonstrate the comparative study of ultimate tensile strength for SMAW & GTAW welded samples. GTAW technique provides sound weld and in these joints samples were fractured along AISI 1040 side. While in SMAW joints fracture was in region of weld bead or at the interface of AISI 1040 and weld bead. The reason behind large difference in ultimate tensile strength of SMAW and GTAW samples may be more stress concentration areas (i-e porosity and slag inclusion) present in the weld bead or interface of the weld bead and AISI 1040 interface.

Black spots in Figure 2 show the presence of porosity and inclusion in SMAW joints at the interface of AISI 1040 and weld zone that may lead towards the lower UTS and yield strength.

Figure 3 shows the comparison for yield strengths of SMAW and GTAW joints. It is clear from Figure 3 that the yield strength of GTAW joints is higher as compared to SMAW joints.

Figure 4 represents the ductility of SMAW and GTAW joints in terms of %age elongation. Ductility of the SMAW joints is very less as compared to the GTAW joints. The maximum value of ductility obtained from the SMAW welded joints is approximately half when compared to the minimum ductility obtained from the

Table 1: Chemical Compositions of Base metals and welding electrodes

Element	C	Si	Mn	P	S	Cr	Ni	Mo	V	Ti	Nb	Fe
ER-309L	0.1	0.36	1.6	<0.01	<0.01	23.8	13	0.06	0.05	0.09	0.01	Balance
E-309 16	0.08	0.52	1.70	0.024	0.021	23.5	12.3	--	--	--	--	Balance
8AISI 1040	0.41	0.14	1.46	<0.05	<0.05		.035	--	--	--	--	Balance
AISI 304	<.07	.41	1.53	.025	.015	18.7	9.34	--	--	--	--	Balance

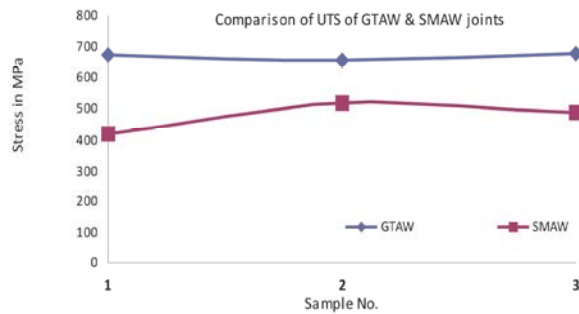


Fig. 1: Comparative analysis of ultimate tensile strength of SMAW and GTAW welded specimens

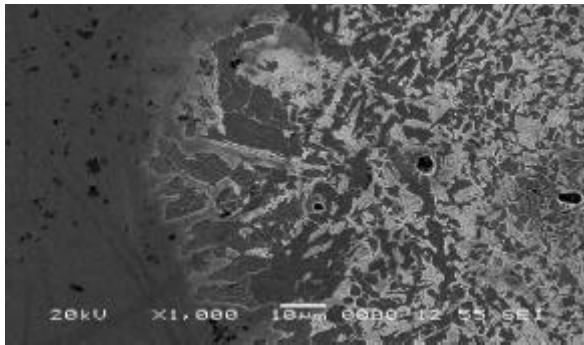


Fig. 2: Presence of porosity and other discontinuities in SMAW.

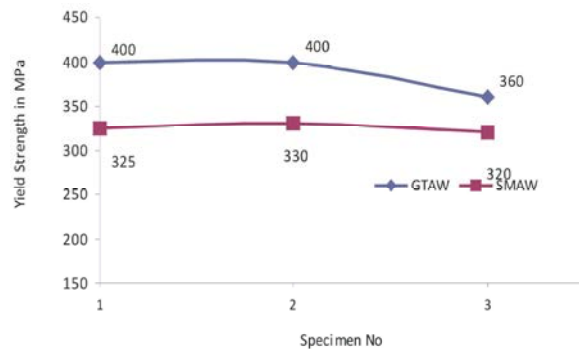


Fig. 3: Comparative analysis of Yield Strength of SMAW and GTAW welded specimens

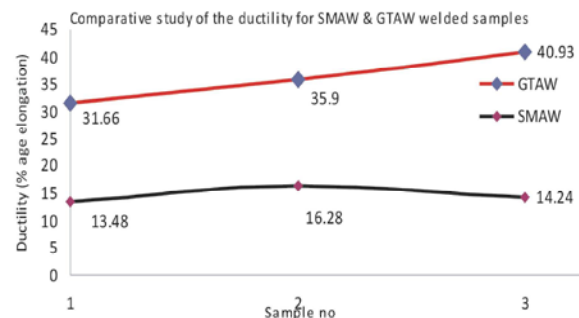


Fig. 4: Linear graph shows the difference in ductility of SMAW and GTAW welded specimens

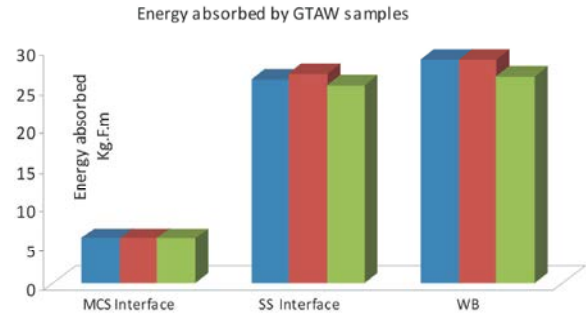


Fig. 5: Three-D Columnar graphs of absorbed energy at different interfaces of specimens welded by GTAW process

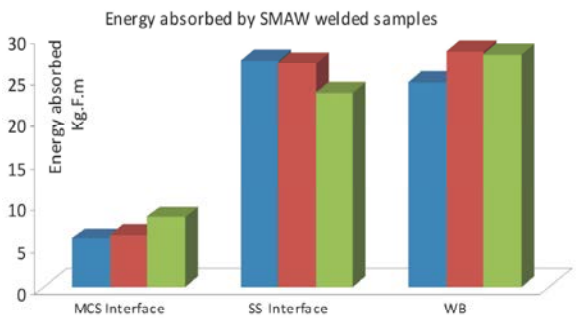


Fig. 6: Three-D Columnar graphs of absorbed energy at different interfaces of specimens welded by SMAW process

GTAW joints. Similarly the maximum value of ductility obtained from the GTAW weld joints is about three times greater as compared to the minimum value of ductility in SMAW joints. In the SMAW welded joints there may be greater chances of the contamination flux of welding electrode if it is not properly cleaned or chipped off and from the atmosphere. Further from the fractured surface, incomplete penetration and porosity was observed. This incomplete penetration leads towards the stress concentration phenomena and failure of the welded joints before reaching its actual UTS value.

Graphs in Figure 5 and Figure 6 show the absorbed energy for GTAW and SMAW samples respectively. Value of impact energy for both techniques is high at the center of weld bead and at the interface of weld zone and AISI 304. Impact energy is low at the interface of AISI 1040 for both SMAW and GTAW joints.

Table 2 shows the bending rate in mm/minute and the bending angle at which crack formation started for SMAW joints. All SMAW joints showed the formation of crack at an angle of 24 degree, 21 degree and 28 degree. Samples prepared from GTAW joints did not illustrate any sign of crack even after bending at an angle of 180°.

Table 2: Bend test results for SMAW joints

ID	Bending Rate mm/min	Result / Breaking Angle
S-1	30	24°
S-2	30	21°
S-3	30	28°

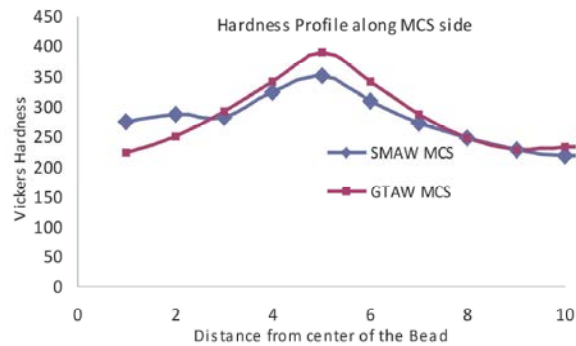


Fig. 7: Hardness profile for SMAW and GTAW along MCS Side

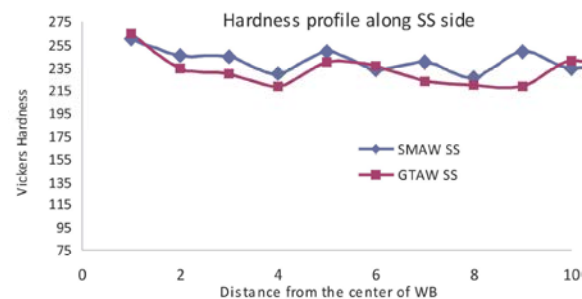


Fig. 8: Profile for hardness from center of WB towards AISI 304 side

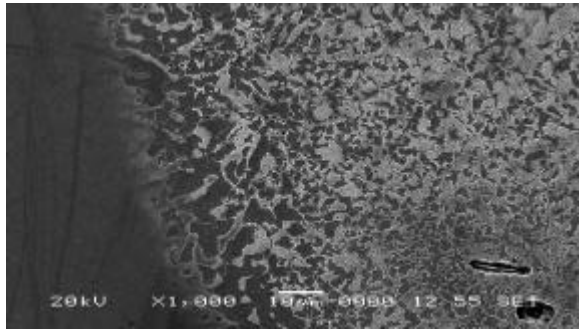


Fig. 9: Microstructure at weld zone

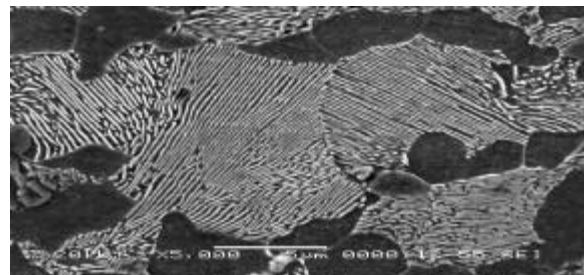


Fig. 10: Microstructure of pearlite.

Further the hardness was measured from centre of the weld zone towards the base metal and passing through the interface and HAZ. Figure 7 provides an idea about the comparative study of hardness profile between the SMAW and GTAW welded joints along AISI 1040 base metal side. The values of maximum Harness are slightly higher in GTAW joints. Hardness profile in GTAW joint is a little bit sharp as compared to the SMAW Joints. Maximum hardness is observed near the interface of weld zone and heat affected zone.

Figure 8 indicates the hardness profile along SS 304 side and there is almost very small or negligible change in the hardness along the AISI 304 side, because AISI 304 is an austenitic grade stainless steel and its hardness cannot be enhanced by the heat treatment process.

Figure 9 reveals the microstructure at the interface of weld zone and AISI 1040 for GTAW welded joints. Microstructure shows that the grain size is large near the weld zone as the temperature in this region reaches near the melting point during welding. The grain size is decreasing gradually as moving from the interface towards the base metal. Very refined grain size is observed in Heat Affected Area near the base metal.

Figure 10 represents the microstructure of pearlite in AISI 1040 showing the alternate layers of ferrite (black) and cementite (white lines).

In Figure 11 white needle like appearance in the base material of AISI 1040 near HAZ is due to presence of sulfur as the EDS analysis of this area showed about 31 % of sulfur. The contents of Sulfur present in the steel is mostly entrapped in the inclusions or grain boundaries in the form of iron sulfide (FeS) due to its low melting point.

EDS analysis also show the dilution of chromium and nickel at the interface of AISI 1040 and weld zone.

Figure 12 shows the microstructure of welded sample (polished with out of electroplating) along AISI side. Composition of Pebble like appearance was analyzed by EDS. Results showed that theses pebbles are corrosion product that is iron oxide.

Figure 13 shows the formation of oxide in welded area and it is maximum at the triple point (where the grain boundaries of three grains are joining) that is the highest energy area. Grain boundaries are also attacked by the corrosion. Centre of black spots in Figure 13 contains some sort of inclusions or porosity, corrosion rate at these spots is low as compared to the grain boundaries.

Figure 14 shows the microstructure of cadmium plating. Thickness of coating is in the range of 16 to 22 micron.



Fig. 11: Needle like structure inside the inclusion indicates entrapment of sulphur.

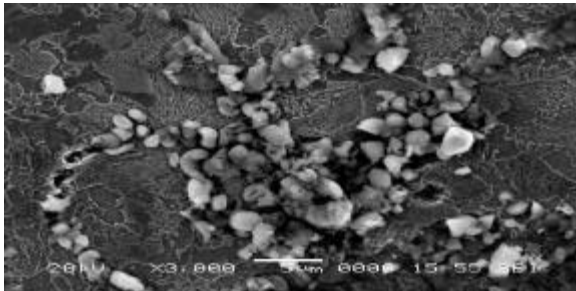


Fig. 12: Microstructure of oxide at the grain boundaries in AISI 1040.



Fig. 13: Microstructure showing the formation of oxide in AISI 1040.

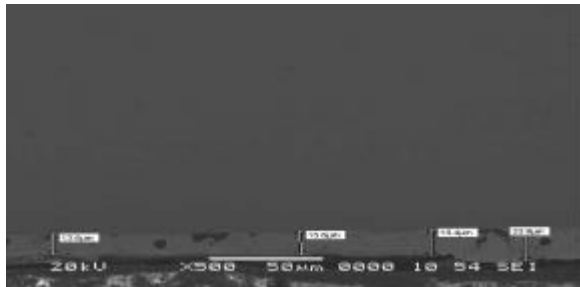


Fig. 14: Manifestation of coating thickness at different locations On SMAW welded sheets

Cadmium electroplated welded sheets were examined in salt spray test and after 96 hours in this test there were no signs of corrosion. Initially it was considered that the

coupling of SS AISI 304 and AISI 1040 is very dangerous because it gives rise to the galvanic corrosion. But coupling of the SS AISI 304 and AISI 1040 followed by the cadmium coating provides complete protection against galvanic and as well as environmental corrosion.

CONCLUSIONS

Following conclusions were made after going through experimentation.

- From mechanical testing made so far it is observed that Weld joint produced by the GTAW process is more reliable as compared to the SMAW technique.
- Tensile properties like UTS, fracture strength, ductility (%age elongation and %age reduction in area) are better in the GTAW process.
- Hardness profile was only observed while moving from the centre of weld bead towards the AISI 1040 side. Value of maximum hardness in the HAZ along AISI 1040 is greater in the GTAW technique because in this process less heat is dissipated consequently high temperature gradient is achieved and this results in the high cooling rate, as compared to the SMAW process. Hardness value in HAZ and interface along the AISI 304 steel almost remains the same, because AISI 304 is an austenitic stainless steel and its hardness cannot be enhanced by the heat treatment process.
- As the temperature near the weld bead is higher and grain size near the weld zone in HAZ is coarser and it becomes refine by moving away from the weld zone till the base metal.
- Dilution of the elements like chromium and nickel was observed at the interface of weld zone and heat affected zone along AISI 1040 steel in both SMAW and GTAW. Rapid Galvanic corrosion was detected. The welded sheets were polished and placed in desiccant environment to minimize the corrosion rate, but presence of oxide powder was also evidenced at the grain boundaries on polished surface after the 10 hours along AISI 1040 steel.
- Welded sheets after Cadmium plating did not show any corrosive symptoms even after salt spray test of 96 hours. Similarly, face bend test was failed for SMAW joints but it was successful for the GTAW joints.

Keeping in view the all observations and results it is concluded that GTAW technique is better than SMAW while welding dissimilar metals for any particular application.

REFERENCES

1. Zhu, M.L. and F.Z. Xuan, 2010. Effects Of Temperature On Tensile And Impact Behavior Of Dissimilar Welds Of Rotor Steels pp: 3346-3352 Materials and Design 31 (2010)
2. Chang, C.C., C.P. Chou, S.N. Hsu, G.Y. Hsiung and J.R. Chen, 2010. Effect of Laser Welding on Properties of Dissimilar Joint of Al-Mg-Si and Al-Mn Aluminum Alloys J. Mater. Sci. Technol., pp: 276-282.
3. Coelho, R.S., A. Kostka, J.F. Santos and A. Kaysser-Pyzalla, XXXX. Friction-stir dissimilar welding of aluminium alloy to high strength steels: Mechanical properties and their relation to microstructure Materials Science & Engineering A (in process)
4. Das, C.R., A.K. Bhaduri, G. Srinivasan, V. Shankar and S. Mathew, 2009. Selection of filler wire for and effect of auto tempering on the mechanical properties of dissimilar metal joint between 403 and 304L(N) stainless steels, Journal of Materials Processing Technology, 209: 1428-143.
5. Wang, S., Q. Ma and Y. Li, 2011. Characterization of microstructure, mechanical properties and corrosion resistance of dissimilar welded joint between 2205 duplex stainless steel and 16MnR” Materials and Design, 32: 831-837.
6. Zettler, R., F. Potomati, J.F. Dos Santos and N.G. Alcantara, 2006. Temperature evolution and mechanical properties of dissimilar friction stir weldments when joining aa2024 and AA7075 with an AA6056 alloy, Welding World 50(11/12): 107-116.
7. Miyazaki, M. and K. Nishio, 1990. Weld. J., 69: S362.
8. Gittos, N.F. and M.H. Scott, 1981. Weld. J., 60: S95.
9. Chen, Y.C. and K. Nakata, 2009. Microstructural characterization and mechanical properties in friction stir welding of aluminum and titanium dissimilar alloys Materials and Design, 30: 469-474.
10. Yu-hua, C., N. Quan and K. Li-ming, XXXX. Interface characteristic of friction stir welding lap joints of Ti/Al dissimilar alloys,
11. Dong, H., C. Liao, L. Yang and C. Dong, 2012. Effects of post-weld heat treatment on dissimilar metal joint between aluminum alloy and stainless steel Materials Science and Engineering A, 550: 423-428.
12. Mourad, A-H.I., A. Khourshid and T. Sharef, 2012. Gas tungsten arc and laser beam welding processes effects on duplex stainless steel 2205 properties Materials Science and Engineering A, 549: 105-113.
13. Naffakh, H., M. Shamanian and F. Ashrafizadeh, 2009. Dissimilar welding of AISI 310 austenitic stainless steel to nickel-based alloy Inconel 657 Journal of Materials Processing Technology 209: 3628-3639
14. ASME CODE. Section IX. Welding and Brazing Qualifications. 1998.
15. ASTM E23-02 Standard Test Methods for Notched Bar Impact Testing of Metallic Materials.
16. ASM Handbook. Boiler and Pressure Vessels Code, Vol. IX. American Society for Metal, Ohio 44073. 1998.